What Is the Initial Chemical Precursor of DNA Strand Breaks Generated by Direct-Type Effects?

Shubhadeep Purkayastha and William A. Bernhard*

Department of Biochemistry & Biophysics, University of Rochester, Rochester, New York 14642

Received: April 2, 2004; In Final Form: June 21, 2004

The present study tests the hypothesis that the majority of DNA strand breaks produced by direct-type effects are due to sugar free radical precursors and that these radicals are produced by direct ionization of the sugar−phosphate backbone or by hole transfer to the sugar from tightly bound water. Well-defined crystalline DNA samples of $d(CGCG)_2$, d(CGCACG:GCGTGC), $d(GTGCGCAC)_2$, and $d((GCACGCGTGC)_2$ were irradiated at 4 K, and their free radical dose response determined from 0 to 1800 kGy. A model is proposed that effectively describes the dose response curves. It includes the following parameters: the free radical concentration at saturation C_{max}, the free radical yields G_b and G_s, and the destruction constants k_b and k_s. The subscripts b and s refer to base-centered and sugar-centered radicals, respectively. In each of these systems, the free radical concentration exhibits a remarkable resistance to dose saturation up to at least 1500 kGy. As predicted, $G_b > G_s$, the G_b/G_s ratio varying between 4 and 12. Likewise, $k_b > k_s$, the k_b/k_s ratio varying between 28 and 81. The lower cross-section for destruction of the sugar-centered radicals is consistent with the expectation that they are relatively radiation resistant. G_b/G is between 0.81 and 0.92, indicating that at low doses the bases trap out 80−90% of the total free radical population. The remaining 10−20% are located on the sugar. At high dose, a larger fraction of the radicals are trapped on the backbone as seen from the ratio C_{mxS}/C_{mxB}, which ranges from 3.5 to 8. This unusually late onset of dose saturation closely parallels that observed for strand break products in earlier studies. There is, therefore, a good correlation between the dose response profiles of sugar-trapped radicals and strand breaks. These observations strongly support the hypothesis that sugar radicals are precursors to the majority of strand breaks produced by the direct-type effect in DNA.

Introduction

DNA plays a central role as the major cellular "target" for ionizing radiation, which produces lesions that differ from the continuously occurring endogenous lesions both in the chemical nature and spatial distribution of the damage. The subsequent DNA damage is traditionally grouped into two categories: "direct-type" damage is the composite of the damage arising from direct ionization of DNA or from the transfer of dry electrons and holes to the DNA from the hydration waters surrounding the DNA and the "indirect-type" damage, which refers to the damage caused by the bulk water radicals. It is significant to note that in the nuclear environment of eukaryotic cells where DNA is tightly packed as chromatin and the amount of unbound water is relatively small, a large fraction of the DNA damage is due to direct-type processes.

Indeed, it is estimated that direct-type effects contribute about 40% to cellular DNA damage, whereas the effects of water radicals amount to about 60%.[1] However, Krisch et al. puts that estimate at about 50% of the total contribution.[2] Indirect-type damage is better characterized, both quantitatively and mechanistically, than the direct-type damage.[1,3] Much of the work on measuring direct damage in DNA is focused on the cleavage of the sugar−phosphate backbone, called strand breaks. The significance of this type of lesions lies in the fact that it can be detected with very high sensitivity and has been observed to correlate directly with biological end points. Though there are strong indications that strand breakage is dominated by the direct-type effect at low ($\Gamma < 13.2$ H_2O/nucleotide) hydration,[4] pathways that lead to direct strand breaks are not yet well understood. Sources of damage to the sugar−phosphate backbone could include direct ionization events on the sugar or hydrogen abstraction from the sugar by the base radicals.[5,6] However, the latter only appears to be a minor contributor in hydrated DNA.[7]

Ionizing radiation produces nonspecific ionizations, ionizing DNA components approximately in direct proportion to the number of electrons per atom (Bragg law). A tally of electrons in DNA indicates that 52% of the ionizations should occur on the sugar phosphate backbone, whereas the remaining 48% should be distributed among the bases. A single ionization event creates a hole and an ejected electron. That means 52% of the holes are initially generated on the sugar−phosphate, corresponding to 26% of the initial radicals. EPR spectroscopy, however, has detected very little sugar damage in irradiated DNA. Close, in a recent paper,[8] has offered an explanation for this by demonstrating that, in general, the EPR spectra of sugar radicals are quite broad and relatively featureless and are, thus, difficult to detect in powder or aqueous samples.

Thus, the radical events that follow the initial deposition of energy in DNA trap out a population of radicals on the bases and the sugar phosphate backbone. As discussed earlier, the electrons are captured exclusively on the bases whereas the holes are formed in the bases and the sugar phosphate backbone. The one-electron oxidized sugar phosphate backbone then participates in two competing forward processes: hole transfer to the base stack or formation of a family of neutral sugar radicals by

* To whom correspondence should be addressed. E-mail: William_Bernhard@urmc.rochester.edu. Fax: (585) 275-6007. Phone: (585) 275-3730.

10.1021/jp048539x CCC: $27.50
Published on Web 10/29/2004

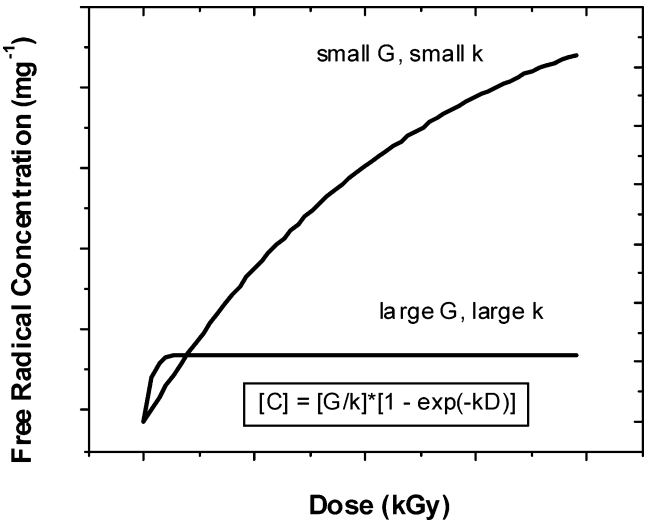

Figure 1. Examples of dose response curves generated from eq 1 illustrating the impact of small *G* and *k* vs large *G* and *k*.

irreversible deprotonation. In older literature, the latter process was assumed to dominate because the free radicals on the sugar moiety were not detected by EPR. However, recent results have pointed out with substantial verity that a significant fraction (~50%) of the holes are irreversibly trapped on the sugar.[9−11]

A recent study by Debije et al. reported the first direct measurement of radiation-chemical yields of specific strand break products induced by the direct effect in X-irradiated crystalline DNA.[10] In this study, the chemical yields of all cleavage fragments that retained at least one unaltered base were determined using HPLC in combination with photodiode array detection. The major products were found to be free bases, and oligodeoxynucleotides with 3′- and 5′-phosphate end groups. The DNA fragmentation pattern was consistent with that predicted for hydrogen abstraction from the sugar phosphate moiety.[12] The accumulation of strand break products was also seen to be remarkably resistant to dose saturation, remaining linear up to unusually high doses of ~500 kGy. These results, in addition to the fact that sugar radicals have been found to be less prone to dose saturation than base-centered radicals support the proposal that direct ionization of DNA gives rise to damaged sugar, presumably sugar-centered radicals that are precursors to strand breaks. It is pertinent in this context to consider other possible precursors to strand breaks that may not generate free radical intermediates detectable by EPR. In recent work, Sanche and collaborators have shown that low-energy electrons (<20 eV) produce strand breaks in plasmid DNA by dissociative electron attachment (DEA). A process by which the majority of secondary electrons generated in the radiation track in the low-energy range 0−30 eV can fragment the ring of thymine and cytosine through resonant interactions.[13−16]

Although EPR detection of sugar radicals has been difficult in general because of their poorly resolved hyperfine structure, evidence for sugar radicals in DNA have emerged nonetheless. Becker and co-workers observed sugar radicals in DNA exposed to high LET radiation.[17] Swarts et al. observed free base release in DNA[18] and Razskazovskiy et al. demonstrated that there is a sizable amount of base release in X-irradiated oligodeoxynucleotide crystals of DNA and that this base release must be due to sugar-centered radicals.[11] And more recently, Debije has identified a 3′-centered sugar radical in crystalline d(CTCTCGAGAG), a B-form DNA X-irradiated at 4 K.[9]

If sugar-centered radicals are indeed the primary precursors to strand breaks, and as seen from the dose saturation characteristics of the strand break fragments,[19] are indeed resistant to radiation destruction, this precursor should then be detectable in a dose response curve extended to very high dose regimes. Upon irradiation, all DNA samples give an initial linear response in the concentration of trapped radicals; however, at some point, the radical concentration reaches a limiting value at which further incident radiation begins to destroy as well as produce radicals. This phenomenon is termed dose saturation. Different chemical species demonstrate different dose saturation characteristics and this is referred to as "saturation asymmetry".[20]

The expression

$$dC/dD = G - kC \quad (1)$$

describes the relationship between the free radical concentration, *C*, and the absorbed dose, *D*. *G* is defined as the rate of production of radicals, and *k* is the rate of destruction per unit dose. As postulated by Müller[21,22] and demonstrated by Snipes and Horan,[23] eq 1 represents the constant production and first-order destruction of free radicals.

By integrating eq 1 with respect to dose, the expression

$$C(D) = C_{max}[1 - e^{-kD}] \quad (2)$$

is obtained where $C_{max} = G/k$ is the free radical concentration at saturation. Figure 1 shows two dose response curves generated from eq 1. Curve 1 of Figure 1 depicts a free radical species that dominates the radical population at low dose but, as a consequence of large *k*, becomes less important at high dose. Conversely, the species represented by curve 2 are difficult to detect at low dose but grow in at high dose by virtue of their stability against destruction (small *k*). It thus appears from the perspective discussed above that saturation asymmetry should occur for the radical population in solid-state DNA. Equation 1 should then be expanded to include at least two components. In this model, each component represents a set of radical species that are characterized by different values of *G* and *k*, namely, the base-centered and the sugar-centered radicals. Thus, we have the expression

$$C(D) = (G_b/k_b)[1 - e^{-k_bD}] + (G_s/k_s)[1 - e^{-k_sD}] \quad (3)$$

where G_b and k_b represent the rate of production and the rate of destruction, respectively, for the base-centered radicals, and G_s and k_s represent the same for the sugar-centered radicals. From eq 3, the quantities G_b/k_b and G_s/k_s yield the values C_{mxB} and C_{mxS}, the free radical concentration at saturation of the base-centered and the sugar-centered radicals, respectively. The total free radical yield, *G*, is $G_b + G_s$.

The objective of this study is to test the hypothesis that the majority of DNA strand breaks produced by direct-type effects are due to sugar free radical precursors and that these radicals are produced by direct ionization of the sugar−phosphate backbone or by hole transfer to the sugar from tightly bound water. The approach entails determining the free radical dose response of well-defined crystalline DNA samples irradiated at 4 K. If the primary precursor to strand breaks is indeed a free radical intermediate, then that intermediate should be stabilized at low temperatures and, therefore, be detectable by EPR. Moreover, because strand breaks do not dose saturate up to and beyond unusually high doses,[19] it is expected that the sugar radical concentration would exhibit comparable behavior.

Materials and Methods

Sample Preparation. Crystals of $d(CGCG)_2$, d(CGCACG:GCGTGC), $d(GCACGCGTGC)_2$, and $d(GTGCGCAC)_2$ were

grown using oligodeoxynucleotides purchased from Ransom Hill Bioscience and used without further purification. Crystals were grown following published procedures.[24−27] Both the tetramer d(CGCG)$_2$ and the nonpalindromic hexamer d(CGCACG:GCGTGC) are Z-form DNA, and the duplexes are packed so as to form parallel columns of continuously stacked base pairs. The octamer d(GTGCGCAC)$_2$ and the decamer d(GCACGCGTGC)$_2$ are both A-form DNA and do not exhibit stacking continuity. Crystals were removed from the mother liquor, carefully dried by application of fine paper wicks, and placed in Charles Supper Co. quartz tubes (chosen for the low free radical background produced upon irradiation). Polycrystalline samples of 250−500 μg were used for all the dose response studies.

Data Collection. Samples were irradiated at 4 K in a Janis Dewar setup[28] with X-rays generated by a Varian/Eimac OEG-76H tungsten-target tube operated at 70 keV and 20 mA. The dose rate was 45 kGy/h. The dose regime extended from 0 to ∼1400 kGy for d(CGCG)$_2$, and from 0 to ∼1800 kGy for the rest of the crystal systems. The samples were raised into the EPR cavity and allowed to equilibrate for several minutes before spectra were recorded. All EPR spectra were taken as first derivatives with a Q-band Varian E-12 EPR spectrometer. Data were collected using 1000 points per EPR scan, typically spanning a field width of 400 G. Approximately 300 G of the scan was devoted to the EPR spectrum of the sample, the remainder being devoted to the spectrum of a ruby marker mounted on the inside wall of the sample cavity. Following a simple ramp baseline correction, the spectrum was numerically integrated to obtain the absorption spectrum. This was then baseline corrected and integrated again, yielding the intensity of the absorption. The baseline correction and integration procedures were also carried out on the ruby portion of the EPR spectrum to determine the intensity of the ruby standard. The number of spins in the experimental sample was then obtained from the following expression:

$$[\mathrm{FR}] = A(I/S_S)(S_R/R)$$

where A is the effective number of spins in the ruby standard, I is the integrated intensity of the sample, R is the integrated intensity of the ruby spectrum, and S_S and S_R were the signal gain used to take the sample spectrum and the ruby spectrum, respectively.[29]

Correction for the Quartz Background. Point defects in crystalline quartz have long been known to be precursors to electron and hole centers and have been extensively studied as such.[30,31] Indeed, trapped atomic hydrogen along with other species has been found to act as paramagnetic centers in crystalline quartz.[30−33] In our system, the quartz background becomes significant at doses of 50 kGy and higher. It was necessary, therefore, to correct the sample EPR spectrum for the quartz background at each dose point. The dose response characteristic of the sample quartz tube (Charles Supper Co.) is investigated in a high-dose regime identical to the one employed for the crystalline oligodeoxynucleotides. Figure 2 shows the EPR spectra of a polycrystalline d(CGCG)$_2$ sample in a quartz tube irradiated at 4 K to a dose of 495 kGy against the spectra obtained for the quartz tube alone irradiated under similar conditions to the same dose. The scan width is 100 mT and includes the signal from the ruby standard for either sample. The sharp pair of lines, as seen in Figure 2, is due to trapped atomic hydrogen in crystalline quartz, and show up as expected along with a broader central quartz peak.

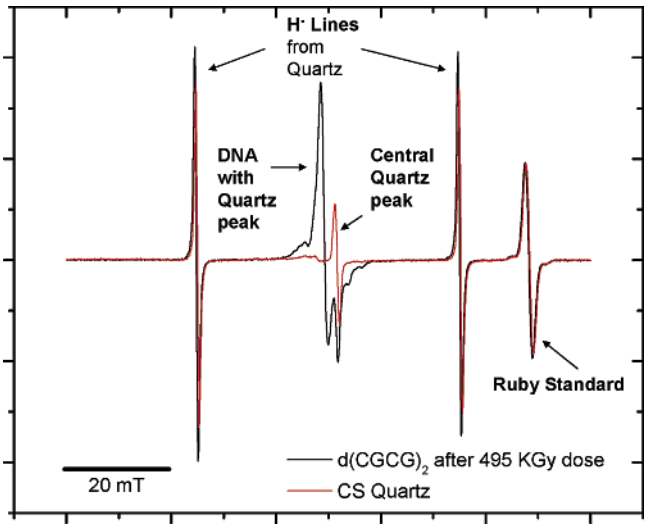

Figure 2. EPR spectrum of a quartz sample tube (red) compared with that of d(CGCG)$_2$ in a quartz tube (black), both X irradiated to a dose of 495 kGy. The scan width was 100 mT, and the spectra were recorded at 4 K. The intensities of the spectra were normalized against the line intensities of the hydrogen atom doublet (hyperfine splitting of 50.7 mT).

Normalized against the average peak-to-peak height of the H$^\bullet$ lines in either spectrum, the area of the central quartz peak is then subtracted from the signal due to DNA plus its quartz container; this is done at each dose point. The free radical concentrations thus obtained were then plotted against the dose to yield the corrected dose response curves, corrected for the quartz background. The corrected dose response curves were then fit to the two-component model discussed earlier using a nonlinear least-squares fitting routine based on the Levenberg−Marquardt method.[34] This method uses the same approach as other standard nonlinear least-squares routines, namely to define a χ^2 merit function and determine best-fit parameters by its minimization. With nonlinear dependences, however, the minimization must proceed iteratively. Given trial values for the parameters, a procedure is developed that improves the trial solution and this procedure is repeated until χ^2 stops (or effectively stops) decreasing.

Results

The corrected dose response curve as obtained for crystalline d(CGCG)$_2$ is shown in Figure 3. It includes both the original curve as well as the one corrected for the quartz background. The dose response curve is then fit to the two-component model given in eq 3. The fitting routine varies any two of the four parameters in eq 3 to assess the appropriateness of the model to the dose response data. The fit to the two-component model yields the parameter values listed in the Table 1. The nonlinear least-squares fit reports the χ^2 and the R^2 (coefficient of determination) values, where R is the correlation coefficient. R^2 is the coefficient of determination expressed as a percentage. The coefficient of determination (COD) indicates how much of the total variation in the dependent variable can be accounted for by the regression function. For example, a COD of 0.70 implies that 70% of the variation in y is accounted for by the regression equation. A COD of 0.7 or higher is considered acceptable for a reasonable model. Based on the goodness-of-fit value as represented by the R^2 parameter, the dose response curve is seen to have a fairly robust fit to the proposed two-component model.

TABLE 1: Parameters G_b, G_s, k_b, and k_s Obtained by Fitting Equation 3 to the Dose Response Curves for Crystalline d(CGCG)$_2$, d(CGCACG:GCGTGC), d(GTGCGCAC)$_2$, and d(GCACGCGTGC)$_2$[a]

sample	G_b (μM/J)	G_s (μM/J)	G_b/G_s	k_b (kGy^{-1})	k_s (kGy^{-1})	k_b/k_s	$10^{-18}C_{mxB}$ (radicals/g)	$10^{-18}C_{mxS}$ (radicals/g)	C_{mxS}/C_{mxB}	G (μM/J)	G_b/G
d(CGCG)$_2$	0.218 (0.003)	0.02 (0.001)	10.9	0.043 (0.001)	0.0011 (0.0001)	39.1	3.1	10.9	3.5	0.238	0.92
d(CGCACG:GCGTGC)	0.425[b] (0.002)	0.036[b] (0.001)	11.8	0.089[b] (0.002)	0.0011[b] (0.0001)	80.9	2.9	19.7	6.8	0.462[b]	0.92
d(GTGCGCAC)$_2$	0.404 (0.007)	0.079 (0.001)	5.1	0.045 (0.001)	0.0011 (0.0001)	40.9	5.4	43.2	8.0	0.482	0.84
d(GCACGCGTGC)$_2$ [high cobalt]	0.382[b] (0.007)	0.08[b] (0.001)	4.8	0.031[b] (0.001)	0.0011[b] (0.0001)	28.2	7.4	43.8	5.9	0.462[b]	0.83
d(GCACGCGTGC)$_2$ [low cobalt]	0.376 (0.008)	0.086 (0.001)	4.4	0.04 (0.001)	0.0014 (0.0001)	28.6	5.7	37.0	6.5	0.462	0.81

[a] The standard errors for each parameter as reported by the nonlinear least-squares fitting procedure are included in the parentheses. The standard errors between different experiments were not determined here, but from previous work[29] the relative error in G values varies from $\pm$5% to $\pm$15% and the absolute error is on the order of 30%. [b] G was set equal to 0.462 μmol/J; G_b, G_s, k_b, and k_s were then scaled to this value of G. See text.

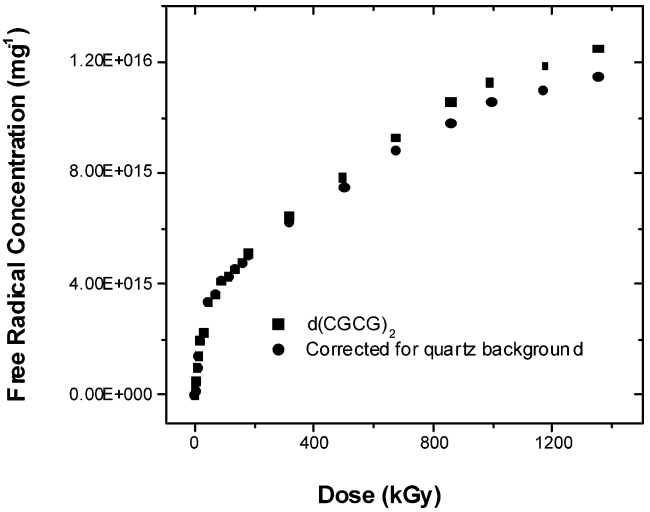

Figure 3. Dose response curve for free radical trapping by d(CGCG)$_2$ in a quartz tube (squares) compared with the curve corrected for the free radical background trapped by the quartz sample tube (circles). X irradiation and EPR measurements were done at 4 K.

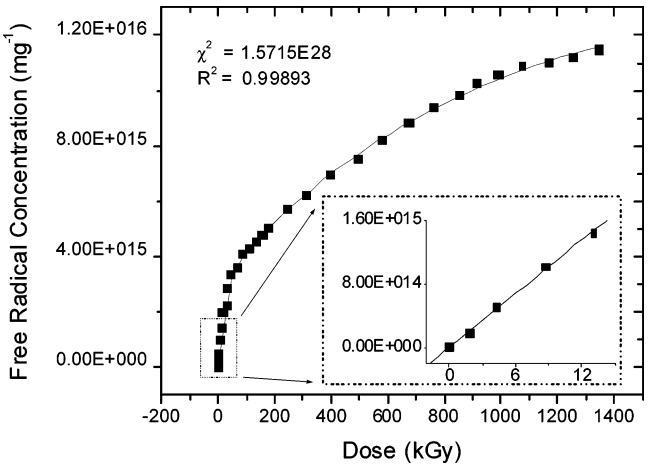

Figure 4. Corrected dose response curve for free radical trapping by d(CGCG)$_2$ fit to the two-component model given in eq 3. R^2 is the goodness of fit, and χ^2 is the reduced χ^2 value calculated by the nonlinear least-squares fitting routine used by ORIGIN. The insert in the figure shows the linear portion of the response in the low-dose regime from which the total free radical yield, G, for the sample is obtained.

Figures 4−8 show the corrected dose response curves as obtained for crystalline d(CGCG)$_2$, d(CGCACG:GCGTGC), d(GTGCGCAC)$_2$, and d(GCACGCGTGC)$_2$ and fit to the proposed two-component model. The best-fit parameter values are listed in the Table 1.

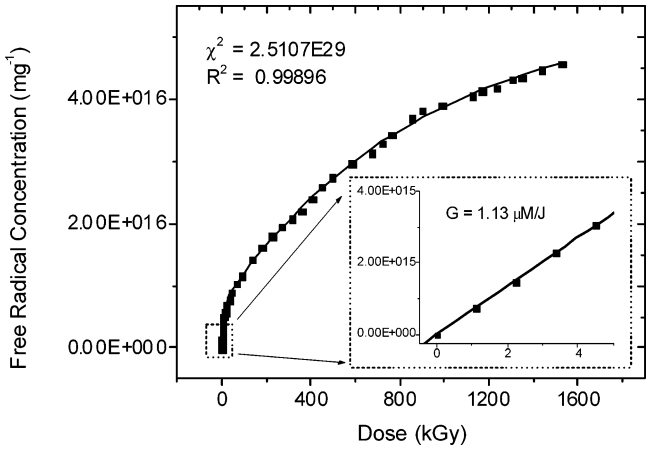

Figure 5. Corrected dose response curve for free radical trapping by d(CGCACG:GCGTGC). Note that the slope shown in the inset (G') is the yield based on exposed dose and not absorbed dose (see text). See Figure 4 caption.

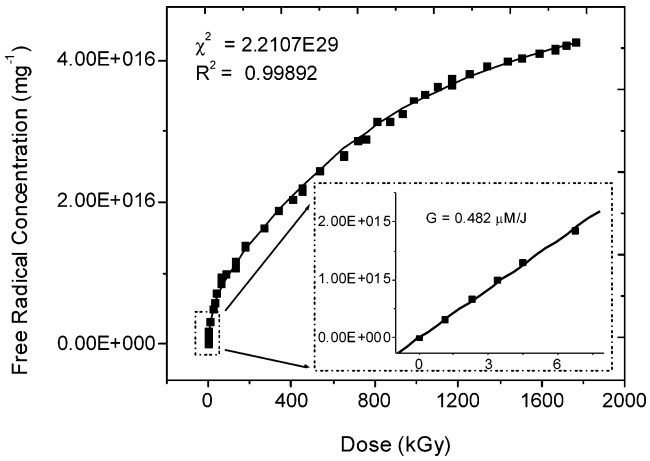

Figure 6. Corrected dose response curve for free radical trapping by d(GTGCGCAC)$_2$ fit to the two-component model. See Figure 4 caption.

The above table summarizes the values of G, k, and C_{max} for the base radical and sugar radical components trapped in the four different types of crystalline DNA. The ratio (G_b/G) represents the fraction of the free radical population located on the base. Likewise, the ratio (G_s/G) is the radical fraction located on the sugar. There are three points related to sample properties that must be noted to compare these values. (i) The absolute yields for crystalline d(CGCACG:GCGTGC) have not been determined because these crystals contain an unknown quantity of barium (used in the crystallization procedure). To facilitate comparison, we assume that the d(CGCACG:GCGTGC) yields are comparable to other crystalline DNAs and assign a value to

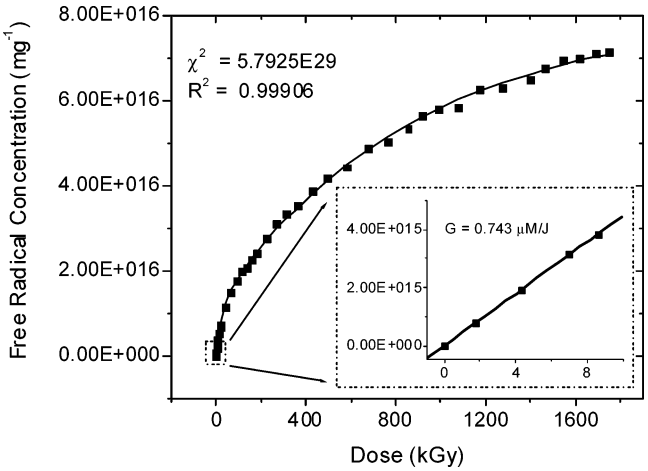

Figure 7. Corrected dose response curve for free radical trapping by d(GCACGCGTGC)$_2$ [high Co] fit to the two-component model. Note that the slope shown in the inset (G') is the yield based on the exposed dose and not absorbed dose (see text). See Figure 4 caption.

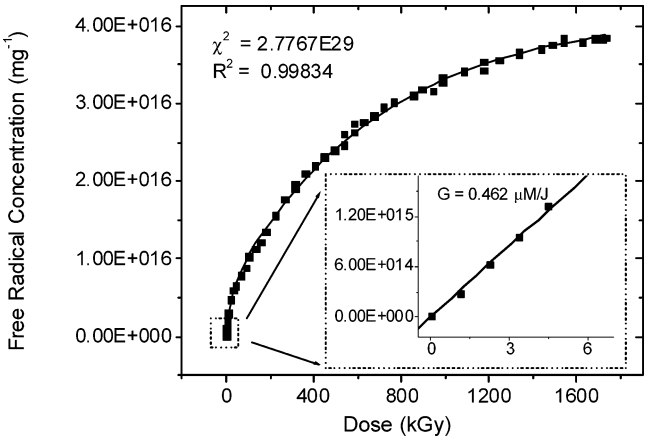

Figure 8. Corrected dose response curve for free radical trapping by d(GCACGCGTGC)$_2$ [low Co] fit to the two-component model. See Figure 4 caption.

G of 0.462 μmol/J. This has no impact on the ratios presented in the Table. (ii) Similarly, the d(GCACGCGTGC)$_2$ crystals contain an unknown amount of cobalt. In this case, the depth of color provides some indication of the level of doping. The sample labeled "high Co" was a deep orange; it gave a yield based on an exposed dose of 0.74 μmol/J. The "low Co" sample was a pale yellow; it gave a yield of 0.46 μmol/J, which is typical for a wide range of crystalline DNAs. We have, therefore, normalized the G and k values of the high-Co sample against $G = 0.46$ μmol/J. (iii) The value of $G = 0.238$ μmol/J measured for d(CGCG)$_2$ is low compared to our earlier published value of 0.65 ± 0.15 μmol/J.[29] After these early studies, we discovered the variability of G measured in crystalline d(CGCG)$_2$ to be far greater than that for any of the other crystalline oligodeoxynucleotides studied to date. In the most recent study, a value of $G = 0.47$ μM/J was obtained for crystalline d(CGCG)$_2$. However, the cause of the variability is not yet determined.

Discussion

A two-component model is found to account for the saturation asymmetry observed in the dose response curves for free radical trapping in crystalline DNA X-irradiated at 4 K. From this we conclude that there are at least two sets of radical species characterized by different values of G and k. Our working hypothesis is that one component consists of free radicals trapped on the bases and the other component consists of radicals trapped on the sugar. In the case of sugar-centered radicals, the cross-section for destruction is smaller than that for base-centered radicals;[17] i.e., they are relatively radiation resistant. This is most likely because the sugar radicals are neutral in charge and the lost proton is displaced a larger distance. The lost proton may attach to a water in the hydration shell or to the DNA bases, e.g., cytosine.[35,36] Either way, the increased distance between the unpaired electron and the site of altered charge helps protect the radical from recombination events.[37] Moreover, the bases serve to protect the sugar-centered holes from electron return on account of being strong electron scavengers. It is also well-known that base-centered electrons and holes are able to transfer between bases.[38−43] As a result, the efficiency of accumulation of radicals on the bases is diminished by the electron/hole mobility between stacked bases. In comparison, the sugar radicals are more deeply trapped due to irreversible deprotonation events, and, consequently, they are immobile. This working model predicts that G_b should be greater than G_s and that k_b should be substantially greater than k_s.

From Table 1, we see that, as predicted, $G_b > G_s$. The G_b/G_s ratio varies from 4 to 12. Likewise, $k_b > k_s$. The k_b/k_s ratio is between 28 and 81. (This is the situation illustrated in Figure 1.) At low doses, G_b/G is between 0.81 and 0.92, indicating that the bases trap out 80−90% of the total free radical population. The remaining 10−20% are located on the sugar. This finding agrees remarkably well with a recent calculation done by Close.[8] At high dose, a larger fraction of the radicals are trapped on the backbone: C_{mxS}/C_{mxB} ranges from 3.5 to 8. This unusually late onset of dose saturation closely parallels that observed for strand break products in earlier studies.[10,19] There is, therefore, a good correlation between the dose response profiles of sugar trapped radicals and strand breaks.

Comparing G and k between different samples we note that the hexamer d(CGCACG:GCGTGC) gives values that deviate to a greater degree than the other compounds. This may well be due to the influence of Ba^{2+}, which doubles the radical concentration per *exposed* dose. Absorption of energy by Ba^{2+} could, therefore, significantly tilt the radical distribution. The excess electrons would most certainly trap out on the bases whereas the hole (Ba^{3+}) should behave much like other holes born in the solvent shell, i.e., transfer to both the bases and sugar. If correct, this would readily explain the large ratios of G_b/G_s and k_b/k_s.

One might expect to observe a similar consequence in the "high Co" vs "low Co" samples of d(GCACGCGTGC)$_2$, as the increased cobalt correlates with an increase in radicals trapped per *exposed* dose (like Ba^{2+}, though less pronounced). But in this case, Co^{3+} has the potential to alter the radical balance in a second way. Unlike Ba^{2+}, Co^{3+} (or quite possibly cobalt(III) hexamine) is a good electron scavenger. It may, thereby, trap a fraction of excess electrons, leaving the ratios of G_b/G_s and k_b/k_s very similar for both the high- and low-Co samples, as is observed. Although evidence of the paramagnetic $Co(NH_3)_6^{2+}$ was not seen in the EPR spectra, this signal would be difficult to detect because the spectrum is expected to be very broad due a nuclear spin of $^7/_2$ and principal g-values that range from 2 to 5. Thus, it is hard to determine to what degree Co^{3+} influences radical trapping by DNA.

Though our results do not prove that the majority of direct-type strand breaks are derived from sugar radicals, they do show that the sugar radical concentration is quantitatively sufficient to explain the majority, perhaps all, of the strand breaks. If a

major source of strand breaks involves intermediates other than free radicals, one must invoke a mechanism by which the observed sugar-centered radicals do NOT lead to strand breaks. That scenario seems improbable. Yet, the proposal that sugar-centered radicals are the major precursor to strand breaks does not in itself rule out the possibility of fragmentation by resonant interactions of low-energy electrons. If, however, LEE play a major role in strand break formation, then free radical intermediates most likely play a role and, therefore, should be observable. Indeed, suggested mechanisms proceed via free radical fragments.[44−46] It would be difficult to distinguish between a set of sugar radicals produced by high-energy (nonresonant) ionization and that by LEE (resonant interaction). But any such fragments, e.g., hydrogen atoms, will be more reactive toward the bases than the sugar. To date, there is no evidence that base radicals are produced in DNA by these types of reactions. Thus, it would appear unlikely that LEE is a major source of strand breaks in directly ionized DNA.

Conclusions

There are two sets of radical species trapped in directly ionized DNA at low temperature; these are distinguished by their different dose response curves. One curve rises quickly (large G) and saturates at low dose (large k). The other rises slowly (small G) and is unusually resistant to dose saturation (small k). The former is assigned to base-centered radicals and the latter to sugar-centered radicals. The cross-section for destruction of the sugar-centered radicals is found to be 25−80 times smaller than that for the base-centered radicals, and the yield is 4−12 times smaller. These observations strongly support the hypothesis that sugar radicals are precursors to the majority of strand breaks produced by the direct-type effect in DNA.

Acknowledgment. We thank Kermit R. Mercer for his invaluable technical assistance. This study was supported by PHS grant 2-R01-CA32546, awarded by the National Cancer Institute, DHHS. Its contents are solely the responsibility of the authors and do not necessarily represent the official views of the National Cancer Institute.

References and Notes

(1) von Sonntag, C. *The Chemical Basis of Radiation Biology*; Taylor and Francis: New York, 1987.
(2) Krisch, R. E.; Flick, M. B.; Trumbore, C. N. *Radiat. Res.* **1991**, *126*, 251.
(3) O'Neill, P. Radiation-induced damage in DNA. In *Radiation Chemistry: Present Status and Future Trends*; Jonah, C. D., Rao, B. S. M., Eds.; Elsevier: Amsterdam, 2001; p 585.
(4) Baverstock, K. F.; Will, S. *Int. J. Radiat. Biol.* **1989**, *55*, 563.
(5) Jones, G. D. D.; O'Neill, P. *Int. J. Radiat. Biol.* **1991**, *59*, 1127.
(6) Catterall, H.; Davies, M. J.; Gilbert, B. C. *J. Chem. Soc., Perkin Trans* **1992**, *2*, 1379.
(7) Swarts, S. G.; Becker, D.; Sevilla, M.; Wheeler, K. T. *Radiat. Res.* **1996**, *145*, 304.
(8) Close, D. M. *Radiat. Res.* **1997**, *147*, 663.
(9) Debije, M. G.; Bernhard, W. A. *Radiat. Res.* **2001**, *155*, 687.
(10) Debije, M. G.; Razskazovskiy, Y.; Bernhard, W. A. *J. Am. Chem. Soc.* **2001**, *123*, 2917.
(11) Razskazovskiy, Y.; Debije, M. G.; Bernhard, W. A. *Radiat. Res.* **2000**, *153*, 436.
(12) Pogozelski, W. K.; Tullius, T. D. *Chem. Rev.* **1998**, *98*, 1089.
(13) Abdoul-Carime, H.; Dugal, P. C.; Sanche, L. *Radiat. Res.* **2000**, *153*, 23.
(14) Abdoul-Carime, H.; Sanche, L. *Radiat. Res.* **2001**, *156*, 151.
(15) Abdoul-Carime, H.; Cloutier, P.; Sanche, L. *Radiat. Res.* **2001**, *155*, 625.
(16) Dugal, P. C.; Huels, M. A.; Sanche, L. *Radiat. Res.* **1999**, *151*, 325.
(17) Becker, D.; Razskazovskii, Y.; Callaghan, M. U. Sevilla. *Radiat. Res.* **1996**, *146*, 361.
(18) Swarts, S. G.; Sevilla, M. D.; Becker, D.; Tokar, C. J.; Wheeler, K. T. *Radiat. Res.* **1992**, *129*, 333.
(19) Razskazovskiy, Y.; Debije, M. G.; Bernhard, W. A. *Radiat. Res.* **2003**, *159*, 663−669.
(20) Spalletta, R. A.; Bernhard, W. A. *Radiat. Res.* **1992**, *130*, 7.
(21) Müller, A. *Int. J. Radiat. Biol.* **1963**, *6*, 137.
(22) Müller, A. *Int. J. Radiat. Biol.* **1964**, *8*, 131.
(23) Snipes, W.; Horan, P. K. *Radiat. Res.* **1967**, *30*, 307.
(24) Crawford, J. L.; Kolpak, F. J.; Wang, A.; Quigley, G.; van Boom, J.; van der Marel, G.; Rich, A. *Proc. Natl. Acad. Sci. U.S.A.* **1980**, *77*, 4016.
(25) Ban, C.; Sundaralingam, M. *Biophys. J.* **1996**, *71*, 1222.
(26) Sadasivan, C.; Gautham, N. *J. Mol. Biol.* **1995**, *248*, 918.
(27) Bingman, C.; Li, X.; Zon, G.; Sundaralingam, M. *Biochemistry* **1992**, *31*, 12803.
(28) Mercer, K. R.; Bernhard, W. A. *J. Magn. Reson.* **1987**, *74*, 66.
(29) Debije, M. G.; Bernhard, W. A. *Radiat. Res.* **1999**, *152*, 583.
(30) Weil, J. A. Muon Resonance: An Application to Study of Hydrogen Position in Quartz. In *Advanced Mineralogy*; Marfunin, A. S., Ed.; Springer-Verlag: Berlin, Germany, 1994; p 227.
(31) Weil, J. A. A Review of the EPR Spectroscopy of the Point Defects in Alpha-Quartz: The Decade 1982−1992. In *The Physics and Chemistry of SiO_2 and the Si−SiO_2 Interface: 2*; Helms, C. R., Ed.; Plenum Press: New York, 1993; p 131.
(32) Leyderman, A.; Weil, J. A.; Williams, J. A. S. *J. Phys. Chem. Solids* **1985**, *46*, 519.
(33) Perlson, B. D.; Weil, J. A. *J. Magn. Reson.* **1974**, *15*, 594.
(34) Marquardt, D. W. *J. Soc. Ind. Appl. Math.* **1963**, *11*, 431.
(35) Wang, W.; Sevilla, M. D. *Radiat. Res.* **1994**, *138*, 9.
(36) Debije, M. G.; Close, D. M.; Bernhard, W. A. *Radiat. Res.* **2002**, *157*, 235.
(37) Bernhard, W. A.; Barnes, J.; Mercer, K. R.; Mroczka, N. *Radiat. Res.* **1994**, *140*, 199.
(38) Gregoli, S.; Olast, M.; Bertinchamps, A. *Radiat. Res.* **1977**, *70*, 255.
(39) van Lith, D.; Warman, J. M.; de Haas, M. P.; Hummel, A. *J. Chem. Soc., Faraday Trans 1* **1986**, *82*, 2933.
(40) Meggers, E.; Kusch, D.; Spichty, M.; Wille, U.; Giese, B. *Angew. Chem., Int. Ed. Engl.* **1998**, *37*, 460.
(41) Debije, M. G.; Milano, M. T.; Bernhard, W. A. *Angew. Chem., Int. Ed. Engl.* **1999**, *38*, 2752.
(42) Lewis, F. D.; Wu, T.; Liu, X.; Letsinger, R. L.; Greenfield, S. R.; Miller, S. E.; Wasielewski, M. R. *J. Am. Chem. Soc.* **2000**, *122*, 2889.
(43) Debije, M. G.; Bernhard, W. A. *J. Phys. Chem. B* **2000**, *104*, 7845.
(44) Boudaiffa, B.; Cloutier, P.; Hunting, D.; Huels, M. A. *Science* **2000**, *287*, 1658.
(45) Boudaiffa, B.; Hunting, D.; Cloutier, P.; Huels, M. A.; Sanche, L. *Int. J. Radiat. Biol.* **2000**, *76*, 1209.
(46) Boudaïffa, B.; Hunting, D.; Cloutier, P.; Huels, M. A.; Sanche, L. *Radiat. Res.* **2002**, *157*, 227.